Teaching Mathematics Independent Study (TMIS) Repository
Volume 2026

https://math.science.cmu.ac.th/tmis.php

Parametric Equations for Closed-loop Kirigami and Application to Cutting Pattern of Tung Sai Moo

Woraphan Wattana[1] **and Supanut Chaidee**[1,*]

[1] *Department of Mathematics, Chiang Mai University, Thailand*
e-mail: woraphan.wat@cmu.ac.th
e-mail: supanut.c@cmu.ac.th

Abstract This study presents a mathematical framework for the construction of closed-loop Kirigami patterns. The proposed approach is based on concentric circular layers partitioned by rotational symmetry and represented through parametric equations. By analyzing the geometric relationships among circular arcs, tangent lines, and regular polygons, a unified description of the cutting pattern is obtained. The framework is further applied to the construction of patterns inspired by the traditional Tung Sai Moo design. The resulting model provides a systematic method for generating rotationally symmetric Kirigami patterns and establishes a mathematical basis for their geometric representation. The proposed framework may be extended to other classes of Kirigami-inspired designs and related geometric structures.

MSC: -

Keywords: Closed-loop Kirigami, Parametric Modeling, Geometric Construction, Rotational Symmetry, Tung Sai Moo

*Corresponding author.

Published by Department of Mathematics, Chiang Mai University.

1. Introduction

Geometry plays an important role in describing patterns, symmetry, and structural forms arising in both mathematics and design. In particular, Kirigami, as an art and geometric construction involving cutting and folding, has attracted increasing attention due to its connections with mathematical modeling, deployable structures, and engineering applications [7, 8].

In 2021, Yue Sun et al. [4] discussed the significance and applications of Kirigami, a traditional paper-cutting art that enables the transformation of flat sheets into complex three-dimensional structures. Kirigami has been widely applied in various fields, including mechanics, materials science, electronics, and bioengineering. They classified Kirigami into two main categories: (1) cutting-only Kirigami and (2) Kirigami involving both cutting and folding. Furthermore, these patterns can be categorized into several types, including fractal, ribbon, lattice, zigzag, and closed-loop Kirigami. Each type exhibits distinct geometric and mechanical characteristics, providing diverse structural behaviors and applications.

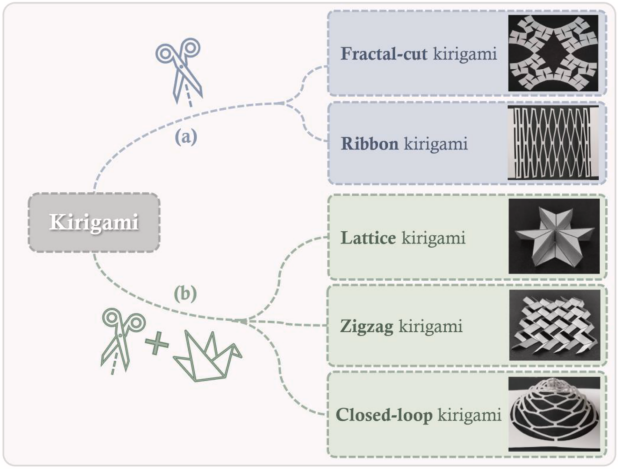

Figure 1. Classification of Kirigami patterns into several types, including fractal, ribbon, lattice, zigzag, and closed-loop Kirigami [4].

Kirigami, the art of cutting and folding materials, has attracted significant attention in recent years due to its ability to transform planar sheets into complex three-dimensional structures. This capability has led to applications in engineering, materials science, and deployable structures [4, 7, 8]. In particular, kirigami-based designs have been widely explored for their mechanical adaptability and structural flexibility [15, 16].

Among various forms of Kirigami, closed-loop Kirigami exhibits distinctive geometric characteristics involving concentric circles, rotational symmetry, and layered cutting structures. These characteristics suggest that closed-loop Kirigami can be analyzed through Euclidean geometry and represented analytically using parametric equations.

Tung Sai Moo, also known as Tung Phaya Yo, is a traditional Lanna auspicious banner used in religious ceremonies, particularly during the Songkran festival and the end of Buddhist Lent [9, 10]. It is commonly offered as a form of merit-making and is often

displayed on sand stupas together with other new year banners. According to Lanna beliefs, such offerings are associated with spiritual merit and the aspiration for rebirth in the era of the Maitreya Buddha.

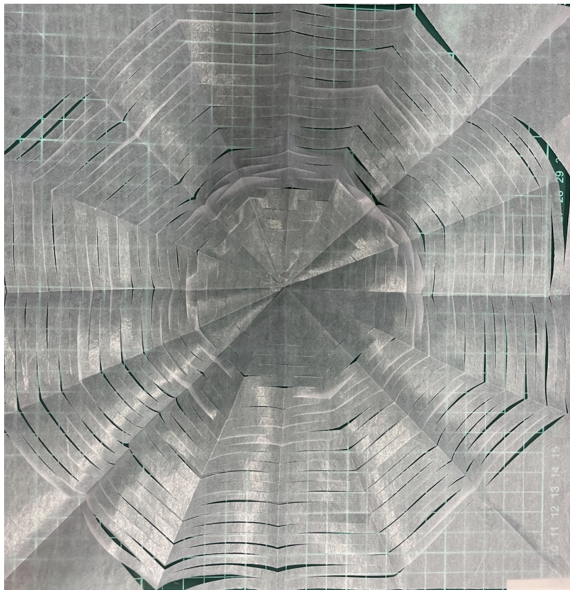

(A) Unfolded Tung Sai Moo pattern under tensile deformation.

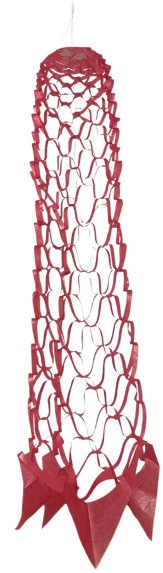

(B) Resulting three-dimensional configuration.

FIGURE 2. Transformation of the Tung Sai Moo pattern from a planar configuration to a three-dimensional structure under tensile deformation.

Geometrically, the construction of Tung Sai Moo involves folding layers of paper diagonally and applying alternating cuts along the folded edges. When unfolded, the pattern forms a continuous and symmetric design, often resembling floral or net-like structures. This process illustrates how simple operations—cutting and unfolding—can transform a two-dimensional sheet into three-dimensional configuration.

Motivated by these observations, this study aims to establish a mathematical framework connecting closed-loop Kirigami and the cutting pattern of Tung Sai Moo through parametric equations and geometric analysis.

The objectives of this study are as follows:

(1) To formulate two-dimensional parametric equations for closed-loop Kirigami and establish associated geometric properties.
(2) To apply these geometric properties to the mathematical approximation of the Tung Sai Moo cutting pattern.

2. Preliminaries

Definition 2.1 (Concentric Circles)**.** A system of concentric circles is a collection of circles that share a common center while having distinct radii. Let O denote the common center and let $r_1 < r_2 < \cdots < r_m$ be the radii of the circles. Then the corresponding circles are called concentric circles.

Definition 2.2 (n-Fold Rotational Symmetry)**.** A figure is said to possess n-fold rotational symmetry about a point O if it remains unchanged after a rotation through an angle $\frac{2\pi}{n}$ about O. Equivalently, the figure coincides with itself after a rotation of one-nth of a full revolution.

Definition 2.3 (Parametric Representation of a Circle)**.** Let $r > 0$ be the radius of a circle centered at the origin. The circle can be represented parametrically by $(x, y) = (r\cos\theta, r\sin\theta)$, where $0 \leq \theta < 2\pi$. Restricting the interval of θ yields an arc of the circle.

Definition 2.4 (**Closed-loop Kirigami**)**.** A closed-loop Kirigami is a class of Kirigami structures in which cuts are introduced into a planar sheet without separating it into disconnected components, such that the structure remains structurally connected. The resulting structure forms a continuous pattern that can be deformed into three-dimensional shapes under external forces.

In this study, a closed-loop Kirigami structure is modeled as a system of concentric circular layers divided into angular partitions. Arc segments are selectively removed according to a prescribed parameter, while the overall connectivity of the structure is preserved [2, 4].

3. Main Results

In this chapter, we present the parametric equation of closed-loop Kirigami and analyze geometry properties for application to cutting pattern of Tung Sai Moo.

3.1. Closed-loop Kirigami Model

3.1.1. Modeling Assumptions

In this section, we define variables based on the cuts made from the Tung Sai Moo method described in the paper. The modeling starts from the closed-loop Kirigami as defined in [4]. We assume that the cutting pattern is derived from concentric circles. Unlike existing approaches that specify the angular parameter θ directly, the present study defines the geometry through the parameter ε, from which θ is subsequently determined. The angular intervals are then defined implicitly through ε which determines the size of the gaps between arc segments. As a result, θ is not treated as an independent variable, but rather as an implicit function constrained by ε and the partition structure of the circle. This formulation provides a more flexible and geometrically meaningful way to control the resulting pattern.

First, let r be the radius of the first layer of cut from the center after the paper is unfolded. The circle is divided into n parts effectively partitioning the angular domain into n intervals. Since the cuts introduce a gap within the circle, the gap is defined by the angular distance ε . This gap also defines the range of angles where the cuts occur. Let θ represent the angular distance at which the cuts are made. The pattern is composed of multiple layers. For each layer, the distance between adjacent cuts corresponds to the inter-circular distance denoted by w. Furthermore, let A denote the number of layers and

let b index the arcs within a given layer. Let r_a denote the radius of the a-th concentric circle layer, where $1 \leq a \leq A$.

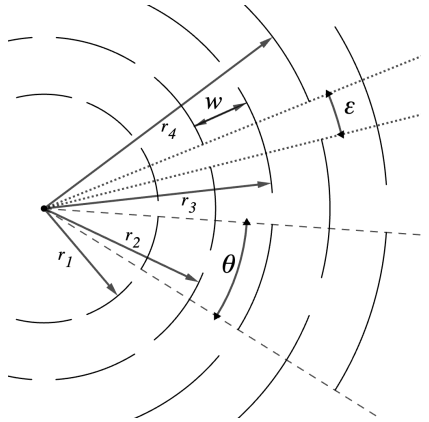

FIGURE 3. Definition of the parameters governing the geometry of the closed-loop Kirigami pattern.

3.1.2. Unified parametric equations for closed-loop Kirigami

To construct the equations of closed-loop Kirigami, we begin with formulating the equation of a circle in a concentric-circle system. For a circle of radius r_a, the polar form is given by

$$(x, y) = (r_a \cos\theta, r_a \sin\theta).$$

Consider a circle partitioned into n equal sectors, each with angular width $\dfrac{2\pi}{n}$, so that initially

$$0 \leq \theta \leq \frac{2\pi}{n}.$$

Let ε denote the total angular gap between adjacent arcs. Since this gap is distributed symmetrically at both endpoints of each arc, each endpoint contributes a gap of $\dfrac{\varepsilon}{2}$.

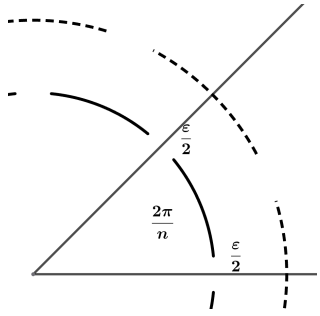

FIGURE 4. An arc with a gap of $\dfrac{\varepsilon}{2}$ removed at the endpoints.

Hence, the angular interval for a single arc is restricted to

$$\frac{\varepsilon}{2} \leq \theta \leq \frac{2\pi}{n} - \frac{\varepsilon}{2}.$$

By shifting the angle successively by $\frac{2\pi}{n}$, the angular intervals for all arcs in a given layer form an arithmetic sequence. Let b index the arcs in a layer, where $1 \leq b \leq n$.

Then the angular interval corresponding to the b-th arc is

$$(b-1)\frac{2\pi}{n} + \frac{\varepsilon}{2} \leq \theta \leq b\frac{2\pi}{n} - \frac{\varepsilon}{2}.$$

For the subsequent layer, the angular interval is offset by half a sector. Since $\frac{1}{2}\left(\frac{2\pi}{n}\right) = \frac{\pi}{n}$, the shifted interval becomes

$$(b-1)\frac{2\pi}{n} + \frac{\pi}{n} + \frac{\varepsilon}{2} \leq \theta \leq b\frac{2\pi}{n} + \frac{\pi}{n} - \frac{\varepsilon}{2}.$$

Simplifying gives

$$(2b-1)\frac{\pi}{n} + \frac{\varepsilon}{2} \leq \theta \leq (2b+1)\frac{\pi}{n} - \frac{\varepsilon}{2}.$$

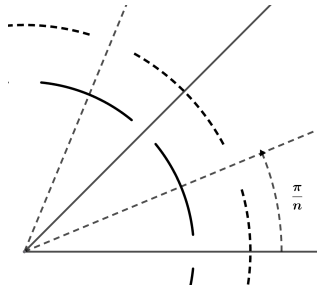

FIGURE 5. Shift angle

Once the initial layer is established, subsequent concentric circle layers are constructed by increasing the radius. Let r_a denote the radius of the a^{th} concentric circle layer. The sequence of radii is given by $r_a = r_1 + (a-1)w$ where w is a distance between successive layers and $1 \leq a \leq A$.

By considering the alternating pattern between adjacent layers, the radii of the closed-loop Kirigami can be expressed as follows:
let

$$r_a = r_1 + (a-1)w, \qquad 1 \leq a \leq A.$$

Define

$$\delta_a = \begin{cases} 0, & a \text{ odd} \\ \dfrac{\pi}{n}, & a \text{ even.} \end{cases}$$

Then the closed-loop Kirigami in the a^{th} layer is represented by

$$(x, y) = (r_a \cos\theta,\, r_a \sin\theta)$$

where

$$(b-1)\frac{2\pi}{n}+\delta_a+\frac{\varepsilon}{2}<\theta<b\frac{2\pi}{n}+\delta_a-\frac{\varepsilon}{2}$$

for

$$1\leq b\leq n.$$

3.2. Geometric Properties of the Tung Sai Moo Cutting Pattern

We analyze the characteristics of closed-loop Kirigami in order to approximate the cutting pattern of Tung Sai Moo. Since closed-loop Kirigami consists of concentric circles divided into n sectors with equal arc lengths, its structure is consistent with n-fold rotational symmetry in which the figure returns to its original configuration after n equal rotations. Accordingly, radial lines are introduced to define the boundaries of each sector in the n-fold symmetry.

Given a fixed ray emanating from the center of circle. To define the n-fold symmetry, radial lines are constructed from the center of the circle to form n axes of symmetry. Let r_1 denote an arbitrary radial line selected as the initial axis. The second radial line, r_2, is obtained by rotating r_1 through an angle of $\frac{360^\circ}{n}$. More generally, the remaining radial lines are generated by rotating r_1 through the following sequence of angles:

$$\begin{aligned}
\theta_{r_2} &= \frac{360^\circ}{n}\\
\theta_{r_3} &= 2\cdot\frac{360^\circ}{n}\\
\theta_{r_4} &= 3\cdot\frac{360^\circ}{n}\\
&\vdots\\
\theta_{r_i} &= (i-1)\cdot\frac{360^\circ}{n}
\end{aligned}$$

However, when partitioning n-fold symmetry on a square sheet, the boundary of the paper must also be taken into account. Consequently, the rotational symmetry of the square imposes constraints on the admissible values of n. Hence, the possible values of n for generating n-fold symmetry are given as follows: 2-fold and 4-fold symmetry.

Next, the circular arcs are approximated by line segments tangent to the concentric circles. The tangents are constructed at the intersection points with the angle bisectors obtained by successive rotations namely at angles of $\frac{\pi}{n}$. Each point of tangency is denoted by t_{ij}, where i identifies the corresponding concentric layer and j identifies the corresponding sector in the n-fold partition.

Lemma 3.1. *Let c_i and c_{i+1} be two consecutive circles in a concentric-circle system with common center O. Let $t_{ij}\in c_i$ and $t_{(i+1)j}\in c_{i+1}$ be the points determined by the same angle bisector of the j-th sector in an n-fold partition. If l_{ij} and $l_{(i+1)j}$ are the tangent lines to c_i and c_{i+1} at t_{ij} and $t_{(i+1)j}$ respectively, then l_{ij} is parallel to $l_{(i+1)j}$.*

Proof. Since c_i and c_{i+1} are concentric circles, they have the same center O. The points t_{ij} and $t_{(i+1)j}$ lie on the same angle bisector of the j-th sector as shown in Figure 7. Hence, the radii Ot_{ij} and $Ot_{(i+1)j}$ are collinear.

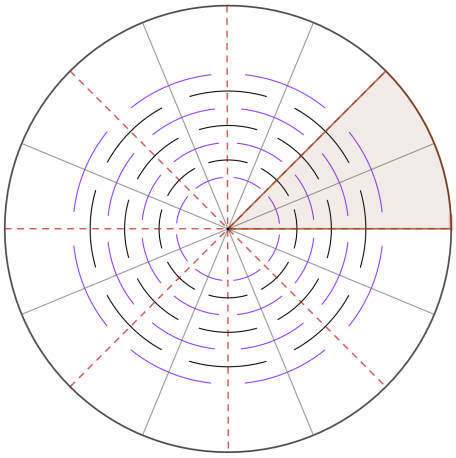

(A) Partitioning 8-fold symmetry on a circular sheet.

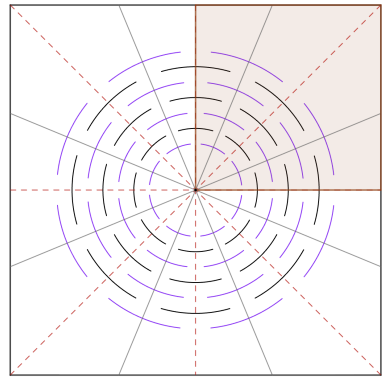

(B) Partitioning 8-fold symmetry on a square sheet.

FIGURE 6. Compare the rotation symmetry of closed-loop Kirigami pattern between the circle paper and square paper.

By the fact that the tangent line to a circle at a given point is perpendicular to the radius drawn to that point, l_{ij} is perpendicular to Ot_{ij} and $l_{(i+1)j}$ is perpendicular to $Ot_{(i+1)j}$. Since Ot_{ij} and $Ot_{(i+1)j}$ are the same line, both tangent lines are perpendicular to the same line. By the converse of Theorem of parallel line, if corresponding angles formed by a transversal are equal, then the two lines are parallel. Therefore, the tangent line l_{ij} is parallel line to the tangent line $l_{(i+1)j}$. ∎

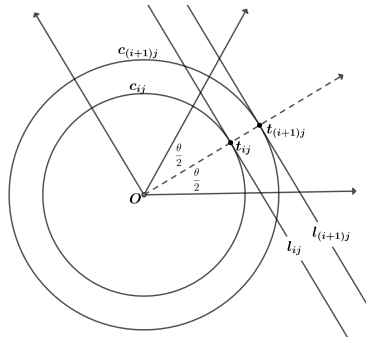

FIGURE 7. Parallelism of tangent lines l_{ij} and $l_{(i+1)j}$ for points of tangency along a common radial line.

Corollary 3.2. *Let $c_1, c_2, \ldots, c_m$ be concentric circles with common center O. For a fixed sector j in an n-fold partition, if $t_{ij} \in c_i$ is the point determined by the corresponding angle bisector, and l_{ij} is the tangent line to c_i at t_{ij}, then all tangent lines $l_{1j}, l_{2j}, \ldots, l_{mj}$ are mutually parallel.*

Proof. For each $i = 1, 2, \ldots, m-1$, lemma 3.1 shows that the tangent line l_{ij} is parallel to the tangent line $l_{(i+1)j}$. By the transitivity of parallelism in the Euclidean plane, it follows that every tangent line l_{ij} is parallel to every other tangent line in the same sector. Hence, all tangent lines corresponding to the same sector are mutually parallel. ∎

Lemma 3.3. *Let $l_1, l_2, \ldots, l_n$ be tangent lines constructed at the points of tangency determined by the n-fold partition of a concentric circle. Let $v_j = l_j \cap l_{j+1}, j = 1, 2, \ldots, n$. Then the points $v_1, v_2, \ldots, v_n$ are the vertices of a regular n-gon.*

Proof. Consider two consecutive tangent lines l_j and l_{j+1}, intersecting at v_j. Since t_j and t_{j+1} are points of tangency, the radii Ot_j and Ot_{j+1} are perpendicular to l_j and l_{j+1} respectively. The figuration is illustrated in Figure 8 . Moreover, $Ot_j = Ot_{j+1}$ since both are radii of the same circle. Since $t_j v_j$ and $t_{j+1} v_j$ are tangent segments, the radii Ot_j and Ot_{j+1} are perpendicular to the tangents at t_j and t_{j+1} respectively. Hence, $\angle Ot_j v_j = \angle Ot_{j+1} v_j = 90°$. Furthermore, Ov_j is common to both triangles. Therefore, the triangles $\triangle Ot_j v_j$ and $\triangle Ot_{j+1} v_j$ are congruent by the RHS congruence criterion.

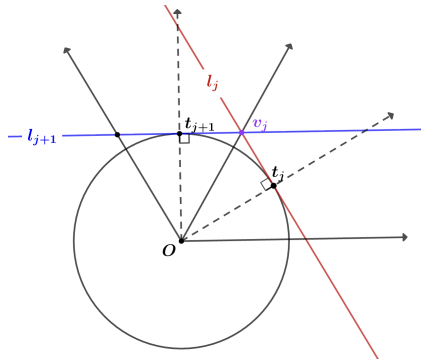

FIGURE 8. Intersection of tangent lines at points v_j illustrating the formation of the vertices of a regular n-gon.

Hence, Ov_j bisects the angle formed by the two tangent lines. Since the central angle between the consecutive points of tangency is $\angle t_j O t_{j+1} = \dfrac{2\pi}{n}$, the angle between the tangent lines is supplementary to this angle. Therefore,$\angle t_j v_j t_{j+1} = \pi - \dfrac{2\pi}{n}$. But this is exactly the interior angle of a regular n-gon since$\dfrac{(n-2)\pi}{n} = \pi - \dfrac{2\pi}{n}$. Since the same argument applies to every consecutive pair of tangent lines, all vertices v_j have equal interior angles. Furthermore, the construction is determined by equal angular increments $\dfrac{2\pi}{n}$, so the resulting sides are equal by symmetry. Therefore, the polygon $v_1 v_2 \cdots v_n$ is a regular n-gon. ∎

Since the tangent lines determine the geometric structure of the approximation and that their intersections form the vertices of a regular n-gon, the next step is to construct parametric equations for the line segments representing the cutting pattern. Since each cut is approximated by a finite segment lying on a tangent line, rather than by the entire tangent line, it is necessary to determine the corresponding parametric representation of these segments.

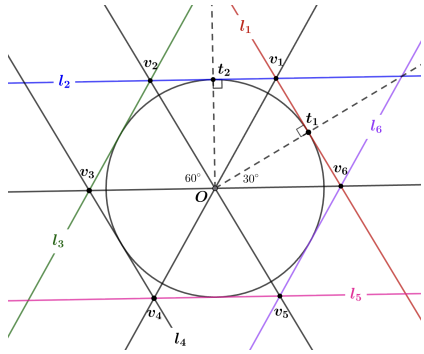

FIGURE 9. Geometric construction of a regular hexagon (6-gon) formed by the intersections v_j of consecutive tangent lines l_j and l_{j+1} on a circle of radius r_i, with a central angle of 60° between adjacent tangency points.

3.3. Conclusion

This study presents a geometric framework for constructing closed-loop Kirigami patterns based on concentric circular layers and rotational symmetry. By introducing a parametric representation of the cutting pattern, a unified mathematical model was developed to describe the geometry of the retained arc segments and their associated line segments.

The proposed framework provides a systematic method for generating closed-loop Kirigami patterns with prescribed geometric properties. Furthermore, the use of tangent-line constructions and regular polygonal structures establishes a clear relationship between the underlying geometric configuration and the resulting cutting pattern.

As an application, the proposed model was employed to construct patterns inspired by the traditional Tung Sai Moo design. The results demonstrate that the geometric characteristics of such patterns can be represented and generated through a parametric approach. The developed framework may serve as a foundation for further studies on the mathematical analysis, design, and optimization of Kirigami-based structures.

References

[1] J. Wang, Y. Zhou, L. Xu, L. Jiang and L. Wang, Magnetic kirigami by laser cutting, Acta Mechanica Solida Sinica 36 (4) (2023) 594–601.

[2] M. Tani, J.-W. Hong, T. Tomizawa, E. Lepoivre, J. Bico and B. Roman, Curvy cuts: Programming axisymmetric kirigami shapes, Extreme Mechanics Letters 71 (2024) 102195.

[3] S. Hoehner, From Circles to Convex Bodies: Approximating Curved Shapes by Polytopes, 2026.

[4] Y. Sun, W. Ye, Y. Chen, W. Fan, J. Feng and P. Sareh, Geometric design classification of kirigami-inspired metastructures and metamaterials, Structures 33 (2021) 3633–3643.

[5] M. Mizuna and E. Iwase, Evaluation Method of Out-of-Plane Deformation on Kirigami Structure with Repetitive Slit Patterns on Concentric Circles, IEEJ Transactions on Electrical and Electronic Engineering 19 (9) (2024) 1579–1583.

[6] R. Fathauer, Tessellations: Mathematics, Art, and Recreation, CRC Press, 2020.
[7] X. Dang et al., Kirigami Engineering: The Interplay Between Geometry and Mechanics, Advanced Materials Reviews (2025).
[8] C.L. Kane and T.C. Lubensky, Topological mechanics of origami and kirigami, Nature Physics 10 (2014) 39–45.
[9] S.J. Tambiah, Tung: Traditional Lanna Banners, Institute of Southeast Asian Studies, 1984.
[10] S. Vallibhotama, Thai Traditions and Cultural Practices, Matichon, 2000.
[11] B. Grünbaum and G.C. Shephard, Tilings and Patterns, W.H. Freeman and Company, New York, 1987.
[12] G.P. Henderson, Parallel Curves, Canadian Journal of Mathematics 6 (1954) 99–107.
[13] E. Schulte, Symmetry of polytopes and polyhedra, in: J.E. Goodman, J. O'Rourke and C.D. Tóth (Eds.), Handbook of Discrete and Computational Geometry, 3rd ed., CRC Press, 2017.
[14] O. Joseph, Pop-Up Geometry, TJ Books Limited, Padstow, Cornwall, United Kingdom, 2022.
[15] H. You, Y. Zhang, Y. Hu, Y. Song, C. Xue, S. Ji, R. Li, L. Li, J. Li, D. Wu and J. Chu, Kirigami structures of shape memory polymer by femtosecond laser scribing and constrained heating, Advanced Materials Technologies 6 (7) (2021).
[16] Z. Liu, H. Du, J. Li, L. Lu, Z. Li and N.X. Fang, Nano-kirigami with giant optical chirality, Science Advances 4 (7) (2018).
[17] H.S.M. Coxeter, Introduction to Geometry, John Wiley & Sons, 1969.